Supporting Information

Counting point defects at nanoparticle surfaces by electron holography

Yan Lu [1, 2], Fengshan Zheng [1], Qianqian Lan [1], Michael Schnedler [1], Philipp Ebert [1], and Rafal E. Dunin-Borkowski [1]

1. *Ernst Ruska-Centre for Microscopy and Spectroscopy with Electrons (ER-C 1) and Peter Grünberg Institute (PGI 5), Forschungszentrum Jülich GmbH, 52425 Jülich, Germany*
2. *Beijing Key Lab and Institute of Microstructure and Properties of Advanced Materials, Beijing University of Technology, Beijing, 100124, China*

1. Experimental procedures

A Cu grid covered on one side by lacey carbon is cut into two halves using a razor blade (reinforced scraper blade), cleaned before in ethanol in an ultrasonic bath for 3 min to remove all surface contaminations. Then the combustion smoke of Mg is collected on all surfaces of the half grid and kept in vacuum until insertion into the TEM holder (within less than a day). This minimizes surface contaminations (hydrocarbons, water) of the MgO nanocubes initially clean directly after combustion.

Prior to the TEM experiments the W tip and the sample holder were plasma cleaned to remove any hydrocarbon contaminations. Then the half grid with the MgO nanocube is installed with previously cleaned tweezers and the holder is loaded into the TEM. In the TEM the W tip is then used to pick up MgO nanocube from the previously cut edge of the Cu grid only (see Fig. S1). Hence the MgO nanocubes investigated did not sit on the lacey carbon and only touched the Cu (the others cannot be reached and picked up by the W tip). Hence, all procedures minimize surface contaminations and the MgO nanocubes should have surfaces essentially free of contaminations during the electron holography experiments.

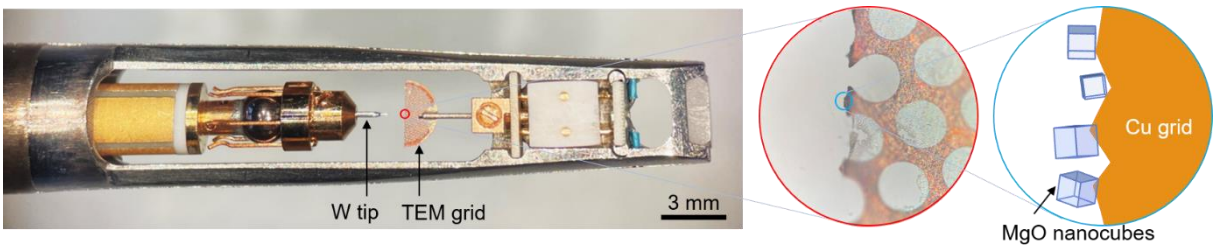

Fig. S1*: NanoFactory STM-TEM holder with W tip to pick up MgO nanocubes sitting on the left side edge of the half Cu grid.*

2. Treatment of errors

A) Sources of systematic errors:
The main sources of systematic errors in the determination of the charge of a nanoparticle is (i) the presence of a W tip used to pick up and manipulate the nanoparticle and (ii) the proximity of a biprism filament used to create a hologram.

(i) The W tip induces a deformation of the centrosymmetric electrostatic potential in its vicinity. This can be well seen in phase maps with isophase lines (Fig. S2). In order to minimize the influence of the

W tip on our results, we extracted the phase profiles in the vacuum (from which the charge is deduced) on the side of the MgO nanocube, which is furthest away from the W tip. The profiles are positioned such that they start from the center of the MgO nanocubes' {100} surface (furthest away from the tip) pointing in normal direction (cf. white arrow in Fig. S2). In this vacuum area the influence of the tip on the potential of the charged MgO nanocube is minimized.

(ii) In addition, the hologram is created by interfering the wave through the nanocube and its vicinity (object wave) with a reference wave passing ideally in a field free region by the nanocube. In reality, the reference wave is still in the region influenced by the Coulomb potential of the charged nanocube and thus in first approximation is affected by a lateral slope in potential. This transfers into an asymmetry in the hologram perpendicular to the biprism filament direction. To minimize the influence of this asymmetry on the measured charge, the tip is positioned roughly parallel to the biprism filament. Thereby the phase change profiles furthest away from the tip, used to deduce the charges, are roughly parallel to the biprism filament, too (Fig. S2). Hence the equi-potential lines in the chosen direction are closest to a centrosymmetric potential compared to any other direction.

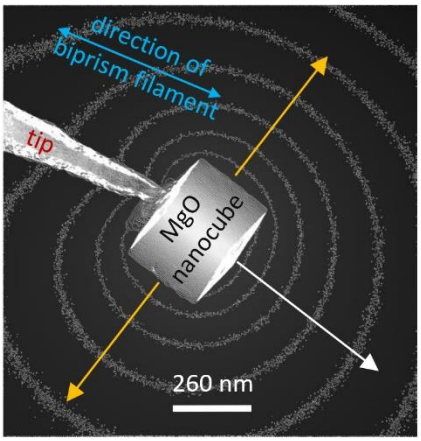

Fig. S2*: Phase map of a MgO nanocube showing phase contours with the contour spacing of 2π/8 (taken from Fig. 1b). The direction of phase change profile used for deducing the charge of the MgO nanocube is indicated by the white arrow. The upper and lower limits of the systematic errors of the charge due to the asymmetry induced by the presence of the biprism and W tip are estimated using perpendicular profiles along the yellow arrows (see text for details).*

B) Estimation of the systematic errors of the charge determination

In order to estimate the effect of the asymmetries induced by the tip and the bisprism on the deduced charge of the MgO nanocubes, we extracted two further line profiles (yellow arrows in Fig. S2) perpendicular to the above mentioned line profile (white arrow in Fig. S2). Along these perpendicular directions, the asymmetric distortion by the biprism is the largest and thus we used the respective profiles for extracting upper and lower limits of the nanocubes' charge.

C) Propagation of errors, fits, and significance of fit models

For the fits shown in Figs. 3 and 4, we treat statistical and systematic errors separately. The systematic errors are due to asymmetries in the phase maps induced by the presence of the W tip and the biprism filament and thus cannot be treated like statistical errors with conventional Gaussian error propagation.

Fit in Fig. 3: Hence, for the fit of the charge vs. electron dose rate data, we performed a chi square minimization without weighting. The *y* intercept of this linear fit provides the immobile charge count.

In order to obtain an upper limit estimate of the systematic error on the charge count, we derived the y-intercepts of linear fits to $y_i+\sigma_{sys,i}^{+}$ and $y_i-\sigma_{sys,i}^{-}$ where $+\sigma_{sys,i}^{+}$ and $-\sigma_{sys,i}^{-}$ are the asymmetric errors in + and $-y$ direction, respectively. This treatment essentially transfers the average systematic error directly to the derived charge count, without reduction due to the number of measurements (as for statistical errors).

In addition to the systematic error, we use the estimated standard error of the y-intercept, as derived by the chi square minimization algorithm, as statistical error of the charge count.

Fit in Fig. 4: For the by chi-square minimization fit of the charge vs. nanocube size data in Figure 4 we treated the systematic and statistical errors in analogy to the above described procedure: The upper and lower limit of the asymmetric systematic errors on the surface and bulk charge densities are estimated using third order polynomial fits to $y_i+\sigma_{sys,i}^{+}$ and $y_i-\sigma_{sys,i}^{-}$ where $+\sigma_{sys,i}^{+}$ and $-\sigma_{sys,i}^{-}$ are the asymmetric systematic errors in + and $-y$ direction. The statistical errors on the surface and bulk charge densities are again obtained by the estimated standard error, derived by the chi square minimization algorithm. The only difference to the fit is Fig.3 is that the individual charge count data points were weighted by their statistical errors in the chi square fit.

We tested three models: Pure bulk, pure surface, and surface plus bulk charge: A pure *bulk* charge model (cubic dependence) is resulting in a coefficient of determination (R^2) of 0.79, which is lower than that of a pure *surface* charge density model (parabolic dependence) of 0.87. The combined model of bulk and surface charge densities has no obvious improvement on the coefficient of determination that is also 0.87, i.e. negligible relative to a pure surface charge density model. This agrees with the fact that the cubic charge density component is below the detection limit, if the error bar is considered as detection limit. Hence, the dominant feature is a surface charge only.

3. Analysis of impurities in the Mg pellets

The following impurities were detected in the Mg pellets used for combustion. The values are given in weight percentage:

Al	0.0226 ± 0.0016
Ca	0.003 ± 0.0007
Fe	0.0024 ± 0.0014
Mn	0.02604 ± 0.00018
Si	0.07 ± 0.04
Zn	0.0042 ± 0.0006

In order to assess if these impurities are really incorporated during combustion, we recall the melting temperature of 2852°C and boiling temperature of 3600°C of MgO. Both are higher than the respective temperatures of the oxides of all found impurities. In particular, the respective temperatures of Mn, Al, and Si oxides are between 600 and more than 2000°C lower and thus it can be anticipated that the impurities will reevaporate from the MgO nanocube at the MgO crystallization temperature. The other impurities incorporated on Mg sites can be expected to exhibit a valence of +2, thus being isoelectronic and not giving rise to charges.